Methylation of (2-Methylethanethiol-bis-3,5-dimethylpyrazolyl)methane Zinc Complexes and Coordination of the Resulting Thioether: Relevance to Zinc-Containing Alkyl Transfer Enzymes

Brian S. Hammes and Carl J. Carrano*

Department of Chemistry and Biochemistry, Southwest Texas State University, San Marcos, Texas 78666

Received October 24, 2000

A series of zinc complexes using a new tripodal, N_2S, heteroscorpionate ligand (L3SH) that is isostructural and isoelectronic with the well-known N_3 trispyrazolylborates have been methylated in solution and the coordination properties of the resulting thioether examined. This system models the reactivity of zinc-containing enzymes involved in alkyl group transfers such as the DNA repair protein Ada from *E. coli*, or farnasyl transferase where it has been shown that the thioether resulting from alkyl group transfer remains in the coordination sphere of the zinc. The following complexes have been structurally characterized: [(L3S)ZnI] (**1**), [(L3SCH$_3$)ZnI$_2$] (**2**), [(L3SCH$_3$)ZnI]BF$_4$ (**3**), [(L3SCH$_3$)Zn-μ-bis-acetato-μ-hydroxo-Zn(L3SCH$_3$)]BF$_4$ (**5**), [(L3SCH$_3$)ZnSPh^{F5}]ClO$_4$ (**7**), and [(L3SCH$_3$)$_2$Zn](BF$_4$)$_2$ (**8**). Complexes **3**, **4**, **5**, **7**, and **8** all display thioether coordination. Thus in the absence of superior anionic ligands, thioethers are reasonably good donors to zinc in either a tetrahedral or octahedral geometry. The methylation of the complex [(L3S)ZnSPh^{F5}], which contains two different thiols, produces a single product, **7**, where only the aliphatic thiol has been alkylated. This observation validates the suggestion that reactivity in enzymes with multiple zinc-bound thiols *could* be controlled by differences in thiol pK_a (Hammes, B. S.; Warthen, C. R.; Crans, D.; Carrano, C. J. *J. Biol. Inorg. Chem*. **2000**, *6*, 82. Compound **7** is also of interest in that it resembles the metal ion-binding site of the blue copper protein, azurin.

Introduction

The role of zinc metalloproteins in enzymatic alkyl group transfer is an emerging area of bioinorganic chemistry.[1] Examples of such enzymes include the DNA repair protein Ada from *E. coli*, the cobalamin dependent and independent methionine synthases, farnasyl transferase, and others.[2−6] In all of these proteins the zinc ion is in a thiol-rich coordination environment with multiple cysteine residues as ligands. Zinc in the Ada protein, for example, is surrounded by four such cysteine residues (designated a CCCC site), although systems in which one or two of the cysteine residues have been replaced by histidines (CCHC and CCHH) are also known.[2−6] Interestingly these same motifs also characterize the nonenzymatic zinc-finger proteins.[1] A major question, which has been addressed by several model compound studies, has been what is the role of the zinc in modulating the reactivity of cysteine residues toward methyl group transfer? In seminal mechanistic work, Wilker and Lippard have shown that in reactions of Zn(SPh)$_4^{2-}$ and its derivatives with trimethyl phosphate as the methyl donor, all the reactivity could be attributed to dissociated thiolate anion.[7] Thus doubts existed regarding the reactivity of a true zinc bound thiolate. More recently, however, both we and Vahrenkamp and associates, have presented evidence for a nondissociative mechanism in the alkylation of [(L)ZnSR] (where L is a trispyrazolylborate or other scorpionate ligand) complexes by a variety of methylating agents.[8,9] The nature of the nucleophile in the enzymatic systems remains ambiguous.[10]

One aspect of the enzymatic reactions not mimicked in any model system studied thus far, however, is the fact that in many of the former, the thioether produced in the alkyl transfer remains coordinated to the zinc. Thioether coordination has been unequivocally demonstrated for the Ada protein, and spectroscopic evidence consistent with this has been presented in several other cases as well.[11−13] Although thioether complexes of zinc are known, in all the model studies involved in alkylation of zinc thiolates, the thioether has never been found in the metals coordination sphere after alkylation.[7−9] This observation has prompted Vahrenkamp to propose that the apparently very poor donor capabilities of the thioether group toward zinc may contribute significantly to the overall reactivity in these systems.[9]

Using a new N_2S heteroscorpionate ligand that is isostructural

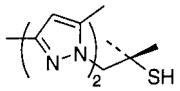

L3SH

and isoelectronic with the well-known N_3 trispyrazolylborates,

(1) Matthews, R. G.; Goulding, C. W. *Curr. Opin. Chem. Biol.* **1997**, *1*, 332.
(2) Friedberg, E. C.; Walker, G. C.; Siede, W. *DNA Repair and Mutagenesis*; ASM Press: Washington, DC, 1995.
(3) Friedberg, E. C. *BioEssays* **1994**, *16*, 645.
(4) Peariso, K.; Goulding, C. W.; Huang, S.; Matthews, R. G.; Penner-Hahn, J. E. *J. Am. Chem. Soc.* **1998**, *120*, 8410.
(5) Zhou, Z. S.; Peariso, K.; Penner-Hahn, J. E.; Matthews, R. G. *Biochemistry* **1999**, *38*, 15915.
(6) Park, H. W.; Boduluri, R. R.; Moomaw, J. F.; Casey, P. J.; Beese, L. S. *Science* **1997**, *275*, 1800.
(7) Wilker, J. J.; Lippard, S. J. *Inorg. Chem.* **1997**, *36*, 969.
(8) Hammes, B. S.; Carrano, C. J. *Inorg. Chem.* **1999**, *38*, 4593.
(9) Brand, U.; Rombach, M.; Vahrenkamp, H. *J. Chem. Soc., Chem. Commun.* **1998**, 2717.
(10) Huang, C.; Hightower, K. E.; Fierke, C. A. *Biochemistry* **2000**, *39*, 2593.
(11) Meyers, L. C.; Cushing, T. D.; Wagner, G.; Verdine, G. L. *Biochemistry* **1993**, *32*, 14089.

10.1021/ic001178p CCC: $20.00
Published on Web 01/25/2001

we report here a system where a zinc-bound thiolate is the active nucleophile, and the thioether resulting from methyl group transfer reaction remains in the coordination sphere of the zinc in the absence of superior anionic ligands. A preliminary account of portions of this work has already appeared.[14]

Experimental Section

All syntheses and crystallizations were carried out under Ar using standard Schlenk or drybox techniques. Solvents dichloromethane and acetonitrile were distilled under argon over CaH_2 while diethyl ether was distilled from Na/benzophenone. All other reagents and solvents were purchased from commercial sources and used as received unless otherwise noted. The ligand L3SH and metal complexes [(L3S)ZnOAc] and [(L3S)ZnSPh^{F5}] were prepared using previously reported procedures.[8]

[(L3S)ZnI] (1). A solution of L3SH (0.78 g, 2.8 mmol) in 30 mL of CH_3OH was treated with NaOMe (0.15 g, 2.8 mmol) under argon. After stirring the solution for 0.5 h, solid ZnI_2 (0.89 g, 2.8 mmol) was added slowly. The resulting solution was stirred for 2 h and filtered to give 0.90 g (69%) of [(L3S)ZnI] as a white solid. Crystals for an X-ray diffraction study were grown by the slow diffusion of hexane into a CH_2Cl_2 solution of [(L3S)ZnI]. Anal. Calcd (found) for [(L3S)ZnI], $C_{14}H_{21}N_4SIZn$: C, 35.80 (35.72); H, 4.52 (4.37); N, 11.93 (11.81). ^{1}H NMR ($CDCl_3$) δ 6.00 (s, 1 H, C*H*), 5.97 (s, 2 H, Pz*H*), 2.51 (s, 6 H, Pz-CH_3), 2.40 (s, 6 H, Pz-CH_3), 1.37 (s, 6 H, C(CH_3)$_2$). ^{13}C NMR ($CDCl_3$) δ 150.42, 140.71, 106.75, 73.10, 48.32, 33.66, 13.84, 11.38.

[(L3SCH$_3$)ZnI$_2$] (2). A solution of **1** (0.49 g, 1.0 mmol) in 30 mL of CH_2Cl_2 was treated with 1 equiv of CH_3I (0.15 g, 1.0 mmol) as a solution in CH_2Cl_2. The resulting reaction mixture was stirred for 1 h, filtered, and concentrated under reduced pressure. Crystallization of the zinc complex was accomplished by layering a concentrated CH_2Cl_2 solution of [(L3SCH$_3$)ZnI$_2$] with isopropyl ether. Over a 3-day period [(L3SCH$_3$)ZnI$_2$] crystallized as colorless blocks (0.38 g, 59%). Anal. Calcd (found) for [(L3SCH$_3$)ZnI$_2$], $C_{15}H_{24}N_4SI_2Zn$: C, 29.45 (29.91); H, 3.96 (3.96); N, 9.16 (9.04). ^{1}H NMR ($CDCl_3$) δ 6.17 (s, 1 H, C*H*), 6.13 (s, 2 H, Pz*H*), 2.62 (s, 6 H, Pz-CH_3), 2.54 (s, 6 H, Pz-CH_3), 1.61 (s, 3 H, S$-$CH_3), 1.41 (s, 6 H, C(CH_3)$_2$). ^{13}C NMR ($CDCl_3$) δ 155.26, 144.80, 108.72, 73.78, 52.12, 26.30, 14.97, 12.43, 11.67.

[(L3SCH$_3$)ZnI]BF$_4$ (3). The tetrafluoroborate salt of [(L3SCH$_3$)ZnI]$^+$ was prepared by two different methods: (A) A solution of [(L3SCH$_3$)ZnI$_2$] (0.30 g, 0.49 mmol) in 25 mL of CH_2Cl_2 was treated with solid $AgBF_4$ (0.096 g, 0.49 mmol). A yellow precipitate was observed following the addition. The resulting solution was stirred for 1 h, filtered to remove the AgI, and concentrated under vacuum. Layering a CH_2Cl_2 solution of [(L3SCH$_3$)ZnI]BF$_4$ with isopropyl ether crystallized the zinc complex, which was filtered and dried under reduced pressure to yield 0.12 g (42%) of [(L3SCH$_3$)ZnI]BF$_4$. (B) A solution of [(L3S)ZnI] (0.27 g, 0.57 mmol) in 25 mL of CH_3CN was treated dropwise with 1 equiv of $(CH_3)_3OBF_4$ (0.085 g, 0.57 mmol) as a solution in CH_3CN. The resulting reaction mixture was stirred for 2 h, filtered, and dried under reduced pressure. Crystallization of the tetrahedral zinc complex was accomplished by slow diffusion of diethyl ether into a concentrated CH_3CN solution of [(L3SCH$_3$)ZnI]BF$_4$. Anal. Calcd (found) for [(L3SCH$_3$)ZnI]BF$_4$, $C_{15}H_{24}N_4SIBF_4Zn$: C, 31.52 (31.62); H, 4.24 (4.17); 9.80 (9.68). ^{1}H NMR (CD_3CN) δ 6.27 (s, 2 H, Pz*H*), 6.21 (s, 1 H, C*H*), 2.48 (s, 6 H, Pz-CH_3), 2.47 (s, 6 H, Pz-CH_3), 1.80 (s, 3 H, $-$SCH_3), 1.28 (s, 6 H, C(CH_3)$_2$). ^{13}C NMR (CD_3CN) δ 154.82, 147.36, 109.41, 72.42, 53.85, 26.84, 15.13, 14.65, 12.68. M$^+$ *m*/*z* 483 (ESI, CH_3OH).

[(L3SCH$_3$)Zn(CH$_3$CN)$_3$](BF$_4$)$_2$ (4). A solution of [(L3SCH$_3$)ZnI$_2$] (0.72 g, 1.2 mmol) in CH_3CN was treated 2 equiv of $AgBF_4$ (0.46 g, 2.4 mmol). A yellow precipitate was observed following the addition of $AgBF_4$. The resulting solution was stirred for 1 h, filtered to remove the AgI, and dried under reduced pressure. The complex was crystallized by vapor diffusion of diethyl ether into a CH_3CN solution of [(L3SCH$_3$)Zn(CH$_3$CN)$_3$](BF$_4$)$_2$ to give 0.45 g (56%). Anal. Calcd (found) for [(L3SCH$_3$)Zn(CH$_3$CN)$_3$](BF$_4$)$_2$·H$_2$O, $C_{21}H_{35}N_7OSB_2F_8Zn$: C, 37.50 (37.48); H, 5.26 (5.05); 14.58 (14.22). ^{1}H NMR (CD_3CN) δ 6.20 (s, 2 H, Pz*H*), 6.11 (s, 1 H, $-$C*H*-), 2.43 (s, 6 H, Pz-CH_3), 2.42 (s, 6 H, Pz-CH_3), 1.97 (s, 6 H, NCCH_3), 1.79 (s, 3 H, SCH_3), 1.28 (s, 6 H, C(CH_3)$_2$). ^{13}C NMR (CD_3CN) δ 153.87, 145.24, 108.67, 70.67, 51.68, 26.42, 14.73, 13.57, 11.86. FTIR (KBr, cm^{-1}): υ_{CN}(NCCH$_3$) = 2288.

[(L3SCH$_3$)Zn-μ-bis-acetato-μ-hydroxo-Zn(L3SCH$_3$)]BF$_4$ (5). The tetrafluoroborate salt of [(L3SCH$_3$)Zn-μ-bis-acetato-μ-hydroxo-Zn(L3SCH$_3$)]$^+$ was prepared by two different methods: (A) A solution of [(L3S)ZnOAc] (0.30 g, 0.75 mmol) in 25 mL of CH_2Cl_2 was treated with 1 equiv of CH_3I (0.11 g, 0.75 mmol) as a solution in CH_2Cl_2. The resulting reaction mixture was stirred for 1 h giving [(L3SCH$_3$)Zn(OAc)(I)]. Without further purification, [(L3SCH$_3$)Zn(OAc)(I)] was treated with a CH_2Cl_2 solution of $AgBF_4$ (0.145 g, 0.75 mmol). A yellow precipitate was observed following the addition. The resulting solution was stirred for 1 h, filtered to remove the AgI, and concentrated under reduced pressure. Layering a CH_2Cl_2 solution of [(L3SCH$_3$)Zn-μ-bis-acetato-μ-hydroxo-Zn(L3SCH$_3$)]BF$_4$ with isopropyl ether crystallized the zinc complex, which was filtered and dried under reduced pressure to yield 0.23 g (41%) of [(L3SCH$_3$)Zn-μ-bis-acetato-μ-hydroxo-Zn(L3SCH$_3$)]BF$_4$ (**5**). (B) A solution of [(L3S)ZnOAc] (0.36 g, 0.89 mmol) in 25 mL of CH_3CN was treated dropwise with 1 equiv of $(CH_3)_3OBF_4$ (0.132 g, 0.89 mmol) as a solution in CH_3CN. The resulting reaction mixture was stirred for 2 h, filtered, and dried under reduced pressure to give **5** as an off-white solid. Crystallization of the zinc complex was accomplished by slow diffusion of diethyl ether into a concentrated CH_2Cl_2 solution of [(L3SCH$_3$)Zn-μ-bis-acetato-μ-hydroxo-Zn(L3SCH$_3$)]BF$_4$ (**5**). Anal. Calcd (found) for [(L3SCH$_3$)Zn-μ-bis-acetato-μ-hydroxo-Zn(L3SCH$_3$)]BF$_4$·CH$_2$Cl$_2$·H$_2$O, $C_{35}H_{59}N_8O_6S_2BF_4Cl_2Zn_2$: C, 40.40 (40.18); H, 5.73 (5.44); N, 10.76 (10.52). ^{1}H NMR (CD_3CN) δ 6.31 (s, 1 H, C*H*), 6.30 (s, 1 H, Pz*H*), 6.15 (s, 1 H, Pz*H*), 2.53 (s, 3 H, Pz-CH_3), 2.51 (s, 3 H, Pz-CH_3), 2.37 (s, 3 H, $-$OC(O)-CH_3), 2.32 (s, 3 H, Pz-CH_3), 1.71 (s, 3 H, SCH_3), 1.63 (s, 3 H, SCH_3), 1.26 (s, 6 H, C(CH_3)$_2$), 1.06 (s, 6 H, C(CH_3)$_2$). FTIR (KBr, cm^{-1}): υ_{CO}(OAc$^-$) = 1612, 1586, 1465, 1424. M$^+$ *m*/*z* 852 (ESI, CH_3OH).

[(L3SCH$_3$)ZnOAc]{*p*-O$_2$N(C$_6$H$_4$)SO$_3$} (6). A solution of [(L3S)ZnOAc] (0.27 g, 0.67 mmol) in 25 mL of CH_2Cl_2 was treated with solid *p*-nitrobenzenesulfonic acid methyl ester (0.15 g, 0.67 mmol). The resulting solution was stirred for 2 h and dried under reduced pressure to give 0.333 g (80%) [(L3SCH$_3$)ZnOAc]{*p*-O$_2$N(C$_6$H$_4$)SO$_3$} as a white solid. Anal. Calcd (found) for [(L3SCH$_3$)ZnOAc]{*p*-O$_2$N(C$_6$H$_4$)SO$_3$}·0.85H$_2$O, $C_{23}H_{32.7}N_5O_{7.85}S_2Zn$: C, 43.54 (43.17); H, 5.21 (4.78); N, 11.04 (10.91). ^{1}H NMR ($CDCl_3$) δ 8.18 (d, 2 H, 8 Hz, Ar*H*), 7.97 (d, 2 H, 8 Hz, Ar*H*), 6.13 (s, 1 H, $-$C*H*-), 6.05 (s, 2 H, Pz*H*), 2.47 (s, 6 H, Pz-CH_3), 2.45 (s, 6 H, Pz-CH_3), 2.10 (s, 3 H, OC(O)-CH_3), 1.67 (s, 3 H, $-$SCH_3), 1.28 (s, 6 H, $-$C(CH_3)$_2$-). ^{13}C NMR ($CDCl_3$) δ 180.82, 153.30, 150.68, 148.25, 143.04, 127.57, 123.33, 107.84, 70.88, 50.69, 25.83, 21.28, 13.77, 13.13, 11.82. FTIR (KBr, cm^{-1}): υ_{CO}(OAc$^-$) = 1524, 1349. M$^+$ *m*/*z* 415 (ESI, CH_3OH).

[(L3SCH$_3$)ZnSPh^{F5}](ClO$_4$) (7). A solution of [(L3S)ZnSPh^{F5}] (0.98 g, 1.8 mmol) in 25 mL of CH_3CN was treated with 1 equiv of CH_3I (0.26 g, 1.8 mmol) as a solution in CH_3CN. The resulting reaction mixture was stirred for 1 h giving [(L3SCH$_3$)Zn(SPh^{F5})(I)]. Without further purification, [(L3SCH$_3$)Zn(SPh^{F5})(I)] was treated with a CH_3CN solution of $AgClO_4$ (0.38 g, 1.8 mmol). A yellow precipitate was observed following the addition. The resulting solution was stirred for 1 h, filtered to remove the AgI, concentrated under reduced pressure, and crystallized by vapor diffusion of diethyl ether into a CH_3CN solution of [(L3SCH$_3$)ZnSPh^{F5}]ClO$_4$ to yield 0.71 g (59%) of [(L3SCH$_3$)-ZnSPh^{F5}]ClO$_4$ (**7**) as colorless blocks. CAUTION! Perchlorate salts can be explosive! Anal. Calcd (found) for [(L3SCH$_3$)ZnSPh^{F5}]ClO$_4$·0.5ACN, $C_{22}H_{25.5}N_{4.5}O_4S_2ClF_5Zn$: C, 38.89 (38.94); H, 3.79 (3.78); N, 9.27 (9.32). ^{1}H NMR (CD_3CN) δ 6.27 (s, 2 H, Pz*H*), 6.18 (s, 1 H, C*H*), 2.48 (s, 6 H, Pz-CH_3), 2.44 (s, 6 H, Pz-CH_3), 1.63 (s, 3 H, $-$SCH_3), 1.21 (s, 6 H, C(CH_3)$_2$). ^{13}C NMR (CD_3CN) δ 153.93, 146.74, 108.53, 71.56, 53.16, 26.06, 14.43, 13.55, 12.06.

[(L3SCH$_3$)$_2$Zn](BF$_4$)$_2$ (8). Allowing a solution of [(L3SCH$_3$)-ZnSPh^{F5}]$^+$ as the tetrafloroborate salt to stand for several days resulted

(12) Ohkubo, T.; Sakashita, H.; Sakuma, T.; Kainosho, M.; Sekiguchi, M.; Morikawa, K. *J. Am. Chem. Soc*. **1994**, *116*, 6035.
(13) Huang, C.; Casey, P. J.; Fierke, C. A. *J. Biol. Chem*. **1997**, *272*, 20.
(14) Carrano, C. J.; Hammes, B. S. *J. Chem. Soc., Chem. Commun*. **2000**, 1635.

in the formation of crystals of the rearrangement product $[(L3SCH_3)_2Zn]BF_4$ (**8**). This material was identified by X-ray diffraction but the small quantity available precluded further analysis.

Physical Methods. Elemental analyses were obtained from Quantitative Technologies, Inc., Whitehouse, NJ. All samples were dried in vacuo prior to analysis. The presence of solvates was corroborated by FTIR, ^{1}H NMR, or X-ray crystallography. ^{1}H and ^{13}C NMR spectra were collected on a Varian UNITY INOVA 400 MHz NMR spectrometer. Chemical shifts are reported in ppm relative to an internal standard of TMS. The ^{13}C quaternary carbon peaks that are not observed are a result of either poor solubility and/or overlapping signals. Electrospray mass spectra (ESI-MS) were recorded on a Finnigan LCQ ion-trap mass spectrometer equipped with an ESI source (Finnigan MAT, San Jose, CA). A gateway PC with Navigator software version 1.2 (Finnigan Corp., 1995−1997), was used for data acquisition and plotting. Isotope distribution patterns were calculated using the program ISOPRO 3.0. IR spectra were recorded as KBr disks on a Perkin-Elmer Spectrum One FTIR spectrometer equipped with a Dell Optiplex PC

Crystallographic Structure Determination. Crystal, data collection, and refinement parameters for [(L3S)ZnI] (**1**), $[(L3SCH_3)ZnI_2]$ (**2**), $[(L3SCH_3)ZnI]BF_4$ (**3**), $[(L3SCH_3)Zn$-μ-bis-acetato-μ-hydroxo-Zn-$(L3SCH_3)]BF_4$ (**5**), $[(L3SCH_3)ZnSPh^{F5}]ClO_4$ (**7**), and $[(L3SCH_3)_2Zn](BF_4)_2$ (**8**), and are given in Table 1. Crystals of all complexes, except (**8**), were sealed in thin-walled quartz capillaries, mounted on a Siemens P4 diffractometer with a sealed-tube Mo X-ray source ($\lambda = 0.71073$ Å) controlled via PC computer. Automatic searching (Siemens XSCANS 2.1), centering, indexing, and least-squares routines were carried out for each crystal with at least 25 reflections in the range, $20° \le 2\theta \le 25°$ used to determine the unit cell parameters. During the data collection, the intensities of three representative reflections were measured every 97 reflection, and any decay observed was empirically corrected for by the software during data processing. Data collection was initiated at 123 K for [(L3S)ZnI] (**1**), 198 K for $[(L3SCH_3)Zn$-μ-bis-acetato-μ-hydroxo-Zn$(L3SCH_3)]BF_4$ (**5**), and 293 K for all others. Crystals of $[(L3SCH_3)_2Zn](BF_4)_2$ (**8**) were mounted on a Nonius Kappa CCD diffractometer and data collected at 123 K. The systematic absences in the diffraction data are consistent with the space groups $P\bar{1}$ for $[(L3SCH_3)ZnI_2]$ (**2**), $P2_1/n$ and $P2_1/c$ for [(L3S)ZnI] (**1**) and $[(L3SCH_3)_2Zn](BF_4)_2$ (**8**), *Pbca* for $[(L3SCH_3)ZnI]BF_4$ (**3**), $P3_221$ for $[(L3SCH_3)Zn$-μ-bis-acetato-μ-hydroxo-Zn$(L3SCH_3)]BF_4$ (**5**), and $C2/c$ for $[(L3SCH_3)ZnSPh^{F5}]ClO_4$ (**7**). The structures were solved using direct methods or via the Patterson function, completed by subsequent difference Fourier syntheses, and refined by full-matrix least-squares procedures on F^2. The metal complexes $[(L3SCH_3)ZnI_2]$ (**2**) and $[(L3SCH_3)_2Zn](BF_4)_2$ (**8**) crystallized with two crystallographically independent, but chemically similar, molecules per unit cell. The metrical parameters quoted in the text refers to only one of the molecules but structural parameters of both crystallographically independent molecules are available in the Supporting Information. The asymmetric unit of $[(L3SCH_3)Zn$-μ-bis-acetato-μ-hydroxo-Zn$(L3SCH_3)]$-$BF_4 \cdot 2H_2O$ (**5**$\cdot 2H_2O$) contains two full molecules of H_2O while the asymmetric unit of $[(L3SCH_3)ZnSPh^{F5}]ClO_4 \cdot 0.5CH_3CN$ (**7**$\cdot 0.5CH_3CN$) contains half of a molecule of CH_3CN located on a special position. All non-hydrogen atoms were refined with anisotropic displacement coefficients and treated as idealized contributions using a riding model except were noted. All software and sources of the scattering factors are contained in the SHELXTL 5.0 program library (G. Sheldrick, Siemens XRD, Madison WI). Selected bond distances and angles for these complexes are shown in Tables2 and 3, and Figures1−6 contain the thermal ellipsoid diagrams.

Results

Molecular Structures

Complexes Containing $(L3S)^-$. The single-crystal X-ray diffraction study of [(L3S)ZnI] (**1**), shown in Figure 1, confirms the tetrahedral coordination geometry around the zinc ion where two pyrazolyl nitrogen donors and one thiolate sulfur donor from $(L3S)^-$ constitute the trigonal face of the tetrahedron. The average $Zn(1)-N_{pz}$ bond length and $N_{pz}-Zn(1)-S(1)$ bond angle is 2.068(5) Å and 97.6(1)°, respectively. The Zn(1)−S(1) bond distance is 2.261(2) Å, in the range seen for many other tetrahedral complexes. The I^- ligand is positioned perpendicular to the trigonal plane formed by the two pyrazolyl nitrogens and the thiolate sulfur of $(L3S)^-$ which results in a Zn(1)−I(1) bond distance of 2.4547(12) Å and average $N_{pz}-Zn(1)-I(1)$ and S(1)−Zn(1)−I(1) bond angles of 119.1(1)° and 127.18(7), respectively. The bond lengths and angles found in [(L3S)ZnI] are not unusual and are similar to those reported previously by us.[8]

Complexes Containing $(L3SCH_3)$. The X-ray structure of the product of the reaction of MeI with **1** is shown in Figure 2. $[(L3SCH_3)ZnI_2]$ (**2**) displays a pseudotetrahedral geometry around the zinc where only the two pyrazolyl nitrogen donors of $(L3SCH_3)$ and two I^- ions are coordinated. Consistent with previous work, the very long average Zn−S distance of 4.4 Å shows clearly that the methylated sulfur atom, of $(L3SCH_3)$, is *not* coordinated. The N(1)−Zn(1)−N(3) bond angle in $[(L3SCH_3)ZnI_2]$ is 92.7(2)° with an average $Zn-N_{pz}$ bond length of 2.058(4) Å. The coordinated iodide ions occupy the two remaining coordination sites with average $N_{pz}-Zn(1)-I$ bond angles of 112.8(1)° and near identical Zn(1)−I bond distances of 2.558(1).

In contrast to the uncoordinated thioether observed in **2**, the molecular structures of $[(L3SCH_3)ZnI]^+$ (Figure 3) and $[(L3SCH_3)_2Zn]^{2+}$ (Figure 4) reveal metal bound thioethers and display pseudotetrahedral and pseudooctahedral geometry, respectively, around the zinc. In $[(L3SCH_3)ZnI]^+$, the two pyrazolyl nitrogens and one thioether sulfur from $(L3SCH_3)$ constitute the trigonal face of the tetrahedron. The average $N_{pz}-Zn(1)-S(1)$ bond angle is 90.2(2)°, which is smaller than that in the unmethylated starting complex [(L3S)ZnI]. Both the average $N_{pz}-Zn(1)-S(1)$ and the N(1)−Zn(1)−N(3) bond angles deviate from the 109.5° angle expected for idealized tetrahedral geometry. The average $N_{pz}-Zn(1)$ bond length is also shorter (2.032(7) Å) than that in the zinc−thiolate complex, [(L3S)ZnI]. This is a direct result of the weaker bonding of the thioether sulfur vis a vis a thiolate as reflected in the lengthening of the Zn(1)−S(1) bond from 2.261(2) Å in [(L3S)ZnI] to 2.391(4) Å in $[(L3SCH_3)ZnI]^+$. The thiother $Zn-S_{thioether}$ distance in **4** is very similar to those reported by Parkin or Riorden et al. in related pseudotetrahedral complexes containing this donor group.[15−17] The iodide ion is positioned perpendicular to the trigonal plane formed by the two pyrazolyl nitrogens and the thioether sulfur of $(L3SCH_3)$ which results in a Zn(1)−I(1) bond distance of 2.468(2) Å and a average $N_{pz}-Zn(1)-I(1)$ and S(1)−Zn(1)−I(1) bond angles of 123.4(2)° and 125.85(10)°, respectively.

For $[(L3SCH_3)_2Zn]^{2+}$, which was crystallized as the tetrafluoroborate salt, the molecular structure shows pseudooctahedral geometry about the zinc ion with two pyrazolyl nitrogens and a thioether sulfur from two different tridentate chelating molecules of $(L3SCH_3)$ facially coordinated to the metal ion. The average $N_{pz}-Zn(1)-N_{pz}$ bond angle and $Zn(1)-N_{pz}$ bond lengths are 107.1(1)° and 2.129(3) Å, respectively. The average $Zn(1)-N_{pz}$ bond distances are considerably longer in $[(L3SCH_3)_2Zn]^{2+}$ than in the tetrahedral complex, $[(L3SCH_3)ZnI]$. The thioether sulfur atoms S(1) and S(2) adopt a *cis* configuration (N(5)−Zn(1)−S(1) = 171.2(2)° and N(1)−Zn(1)−S(2) =

(15) Ghosh, P.; Parkin, G. *J. Chem. Soc., Chem. Commun*. **1998**, 413.
(16) Chiou, S.; Ge, P.; Riordan, C. G.; Liable-Sands, L. M.; Rheingold, A. L. *J. Chem. Soc., Chem. Commun.* **1999**, 159.
(17) Chiou, S.; Innocent, J.; Riordan, C. G.; Lam, K.; Liable-Sands, L.; Rheingold, A. L. *Inorg. Chem*. **2000**, *39*, 4347.

Table 1. Summary of Crystallographic Data and Parameters for [(L3S)ZnI] (**1**), [(L3SCH$_3$)ZnI$_2$] (**2**), [(L3SCH$_3$)ZnI]BF$_4$ (**3**), [(L3SCH$_3$)Zn-μ-bis-acetato-μ-hydroxo-Zn(L3SCH$_3$)]BF$_4$·2H$_2$O (**5**·2H$_2$O), [(L3SCH$_3$)ZnSPh^{F5}]ClO$_4$·0.5CH$_3$CN (**7**·0.5CH$_3$CN), and [(L3SCH$_3$)$_2$Zn](BF$_4$)$_2$ (**8**)

	1	**2**	**3**	**5**·2H$_2$O	**7**·0.5CH$_3$CN	**8**
molecular formula	$C_{40}H_{40}I_2N_4O_2SZn$	$C_{15}H_{30}I_2N_4SZn$	$C_{15}H_{24}BF_4IN_4SZn$	$C_{17}H_{27}B_{0.5}F_2N_4O_{2.5}SZn$	$C_{22}H_{24}ClF_5N_{4.5}O_4S_2Zn$	$C_{60}H_{96}B_4F_{16}N_{16}S_4Zn_2$
Fw	959.99	617.66	571.52	468.26	675.40	1647.75
temp (K)	123(2)	293(2)	293(2)	198(2)	293(2)	123(2)
cryst system	monoclinic	triclinc	orthorhombic	trigonal	monoclinc	monoclinic
space group	$P2_1/n$	$P\bar{1}$	$Pbca$	$P3_221$	$C2/c$	$P2_1/c$
cell constants						
a (Å)	8.142(2)	8.370(3)	9.752(2)	17.674(5)	21.078(3)	33.986(7)
b (Å)	22.318(5)	14.983(4)	19.758(3)	17.674(5)	17.597(3)	10.294(2)
c (Å)	10.019(2)	18.428(4)	22.963(3)	15.531(3)	17.096(3)	22.245(4)
α (deg)	90	71.31(2)	90	90	90	90
β (deg)	94.42(3)	80.85(2)	90	90	118.01(2)	106.24(3)
γ (deg)	90	88.99(3)	90	120	90	90
Z	2	4	9	6	8	4
V (Å^3)	1815.0(6)	2159.9(10)	4424.3(13)	4202(2)	5598(2)	7472(3)
abs coeff, μ_{calcd} (mm^{-1})	2.477	4.097	2.970	0.981	1.193	0.844
δ_{calcd} (g/cm^3)	1.757	1.899	1.931	1.110	1.603	1.465
F(000)	952	1200	2538	1461	2748	3424
cryst dimens (mm)	0.7 × 0.5 × 0.6	1.0 × 0.7 × 0.7	0.4 × 0.3 × 0.1	0.5 × 0.5 × 0.3	0.9 × 0.7 × 0.4	0.025 × 0.16 × 0.52
radiation	Mo Kα (λ = 0.71073 Å)	Mo Kα (λ = 0.71073 Å)	Mo Kα (λ = 0.71073 Å)	Mo Kα (λ = 0.71073 Å)	Mo Kα (λ = 0.71073 Å)	Mo Kα (λ = 0.71073 Å)
h,k,l ranges colld	−10 → 10, −28 → 28, −13 → 11	0 → 7, −15 → 15, −19 → 19	0 → 9, −21 → 0, 0 → 24	0 → 18, −19 → 0, −16 → 0	0 → 22, −18 → 0, −18 → 16	−44 → 34, −13 → 13, −24 → 28
θ range (deg)	1.78−22.50	2.13−22.50	1.77−22.49	1.87−22.52	2.19−22.50	2.93−27.51
no. of reflens colld	4499	5685	2635	4025	3773	52127
no. of unique reflens	4198	5215	2635	3522	3656	16283
no. of params	190	415	258	258	359	975
data/param ratio	21.78	12.55	10.21	13.63	10.17	16.70
refinement method	full-matrix least-squares on F^2	full-matrix least-squares of F^2	full-matrix least-squares of F^2	full-matrix least-squares of F^2	full-matrix least-squares of F^2	full-matrix least-squares of F^2
$R(F)^a$	0.0738	0.0379	0.0640	0.0799	0.0610	0.0858
$R_w(F^2)^b$	0.2312	0.0989	0.01607	0.2317	0.1677	0.1716
GOFw^c	1.033	1.086	0.980	1.067	1.045	1.021
largest diff peak and hole (e/Å^3)	3.464 and − 3.101	0.837 and −0.775	0.978 and −1021	1.644 and −0.504	0.942 and −0.926	0.702 and −0.579

[a] $R = [\sum|\Delta F|/\sum|F_o|]$. [b] $R_w = [\sum w(\Delta F)^2/\sum wF_o^2]$. [c] Goodness of fit on F^2.

Table 2. Selected Bond Distances and Angles for [(L3S)ZnI] (**1**), [(L3SCH$_3$)ZnI$_2$] (**2**), [(L3SCH$_3$)ZnI]BF$_4$ (**3**), and [(L3SCH$_3$)ZnSPh^{F5}]ClO$_4$ (**7**)[a]

distance (Å) and angle (deg)	**1**	**2**	**3**	**7**
Zn(1)−N(1)	2.077(7)	2.060(6)	2.025(11)	2.003(5)
Zn(1)−N(3)	2.059(6)	2.055(6)	2.038(10)	2.010(5)
Zn(1)−S(1)	2.261(2)		2.391(4)	2.563(2)
Zn(1)−S(2)				2.227(2)
Zn(1)−I(1)	2.4547(12)	2.5581(12)	2.468(2)	
Zn(1)−I(2)		2.5582(12)		
Zn(1)−O(1)				2.53
N(1)−Zn(1)−N(3)	87.3(3)	92.7(2)	94.1(4)	92.2(2)
N(1)−Zn(1)−S(1)	95.2(2)		90.5(3)	88.28(14)
N(1)−Zn(1)−S(2)				134.7(2)
N(1)−Zn(1)−O(1)				
N(1)−Zn(1)−I(1)	118.4(2)	119.0(2)	122.4(3)	
N(1)−Zn(1)−I(2)		106.6(2)		
N(3)−Zn(1)−O(1)				
N(3)−Zn(1)−S(1)	100.0(2)		90.0(3)	85.26(14)
N(3)−Zn(1)−I(1)	119.7(2)	113.7(2)	124.3(3)	
N(3)−Zn(1)−I(2)		112.0(2)		
N(3)−Zn(1)−S(2)		106.6(2)		131.5(2)
S(1)−Zn(1)−O(1)				
S(1)−Zn(1)−I(1)	127.18(7)		125.85(10)	
S(1)−Zn(1)−S(2)				104.41(6)
S(2)−Zn(1)−O(1)				
I(1)−Zn(1)−I(2)		111.43(4)		
d[Zn−N$_{pz}$, −S(2)][b]				0.147

[a] Numbers in parentheses are estimated standard deviations. [b] Displacement of zinc ion from the plane formed by N(1), N(3), and S(2).

Table 3. Selected Bond Distances and Angles for [(L3SCH$_3$)Zn-μ-bis-acetato-μ-hydroxo-Zn(L3SCH$_3$)]BF$_4$ (**5**) and [(L3SCH$_3$)$_2$Zn][BF$_4$]$_2$ (**8**)[a]

distance (Å) and angle (deg)	**5**	**8**
Zn(1)−N(1)	2.174(9)	2.096(5)
Zn(1)−N(3)	2.118(9)	2.131(5)
Zn(1)−N(5)		2.102(5)
Zn(1)−N(7)		2.187(5)
Zn(1)−S(1)	2.619(3)	2.601(2)
Zn(1)−S(2)		2.641(2)
Zn(1)−O(1)	1.979(4)	
Zn(1)−O(2)	2.157(7)	
Zn(1)−O(3)	2.078(8)	
N(1)−Zn(1)−N(3)	85.1(3)	87.4(2)
N(1)−Zn(1)−N(5)		101.2(2)
N(1)−Zn(1)−N(7)		94.6(2)
N(1)−Zn(1)−S(1)	82.6(2)	87.5(2)
N(1)−Zn(1)−S(2)		167.2(2)
N(1)−Zn(1)−O(1)	96.0(3)	
N(1)−Zn(1)−O(2)	173.5(3)	
N(1)−Zn(1)−O(3)	93.5(3)	
N(3)−Zn(1)−N(5)		99.5(2)
N(3)−Zn(1)−N(7)		171.8(2)
N(3)−Zn(1)−S(1)	87.9(2)	82.2(2)
N(3)−Zn(1)−S(2)		100.8(2)
N(3)−Zn(1)−O(1)	173.0(3)	
N(3)−Zn(1)−O(2)	90.0(3)	
N(3)−Zn(1)−O(3)	92.0(3)	
N(5)−Zn(1)−N(7)		88.0(2)
N(5)−Zn(1)−S(1)		171.2(2)
N(5)−Zn(1)−S(2)		87.3(2)
N(7)−Zn(1)−S(1)		89.94(14)
N(7)−Zn(1)−S(2)		75.95(14)
O(1)−Zn(1)−O(2)		
O(1)−Zn(1)−O(3)		
O(2)−Zn(1)−O(3)		
S(1)−Zn(1)−O(1)	85.3(2)	
S(1)−Zn(1)−O(2)	92.9(2)	
S(1)−Zn(1)−O(3)	176.1(2)	
S(1)−Zn(1)−S(2)		83.88(7)

[a] Numbers in parentheses are estimated standard deviations.

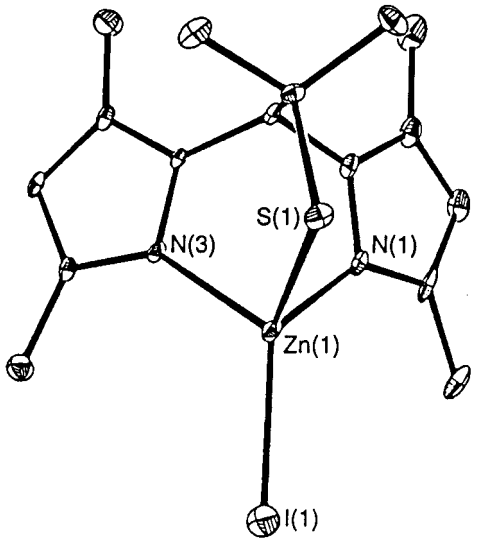

Figure 1. ORTEP diagram with 30% thermal ellipsoids for [(L3S)ZnI] showing atomic labeling for the coordination sphere only. Hydrogen atoms are omitted for clarity.

167.2(2)°) and average Zn(1)−S$_{thioether}$ bond length of 2.621(1) Å. Although the zinc thioether bonds in this six coordinate species are considerably longer than those seen in the 4-coordinate analogue, they are still clearly within bonding distance and are similar to those reported by Riorden.[16,17]

The molecular structure of the six-coordinate dimer [(L3SCH$_3$)-Zn-μ-bis-acetato-μ-hydroxo-Zn(L3SCH$_3$)]$^+$, shown in Figure 5, has pseudooctahedral geometry about both Zn(II) ions with two pyrazolyl nitrogens and a thioether sulfur from one (L3SCH$_3$) coordinated facially to each zinc ion. The N(1)−Zn(1)−N(3)/N(5)−Zn(2)−N(7) bond angles and Zn(1)−N$_{pz}$/Zn(2)−N$_{pz}$ bond lengths are 85.1(3)° and 2.146(6) Å, respectively. The average Zn(1)−N$_{pz}$ bond distances are considerably longer in [(L3SCH$_3$)-Zn-μ-bis-acetato-μ-hydroxo-Zn(L3SCH$_3$)]$^+$ than in the tetrahedral complex, [(L3SCH$_3$)ZnI]$^+$; however, they are consistent with the octahedral complex [(L3SCH$_3$)$_2$Zn]$^{2+}$. The thioether sulfur atom S(1) is *trans* to a bridging acetato (OAc)$^-$ ligand with a S(1)−Zn(1)−O(3) bond angle of 176.1(2)° and a Zn(1)−S(1) bond length of 2.619(3) Å. The Zn(1)−S$_{thioether}$ bond length is virtually the same as that found in **8**. The acetato (OAc)$^-$ ligands in [(L3SCH$_3$)Zn-μ-bis-acetato-μ-hydroxo-Zn-(L3SCH$_3$)] exhibits η^2 coordination to the zinc ions with a symmetric Zn(II)−O$_{acetate}$ bond distance (Zn(1)−O(2) = 2.157-(7) Å and Zn(1)−O(3) = 2.078(8) Å). In addition, a μ coordinated hydroxo moiety was located *trans* to the pyrazolyl nitrogen N(3) with N(3)−Zn(1)−O(1) bond angle of 173.0(3)° and a Zn(1)−O(1) bond length of 1.979. Other bond lengths and angles are not unusual and are similar to those reported for a similar acetate bridged dimer reported by Weighardt.[18]

The solid-state structure of [(L3SCH$_3$)ZnSPh^{F5}]$^+$, shown in Figure 6, shows pseudotrigonal bipyramidal coordination geometry around the zinc ion where the two pyrazolyl nitrogens from (L3SCH$_3$) and the thiolate sulfur from (SPh^{F5})$^-$ are coordinated in the trigonal plane. The N(1)−Zn(1)−N(3) and average N$_{pz}$−Zn(1)−S(2) bond angles are 92.2(2)° and 133.1-(1)°, respectively, which deviate from the 120° angles expected

(18) Chadudhuri, P.; Stockheim, C.; Wieghardt, K.; Deck, W.; Gregorzik, R.; Vahrenkamp, H.; Nuber, B.; Weiss, J. *Inorg. Chem.* **1992**, *31*, 1451.

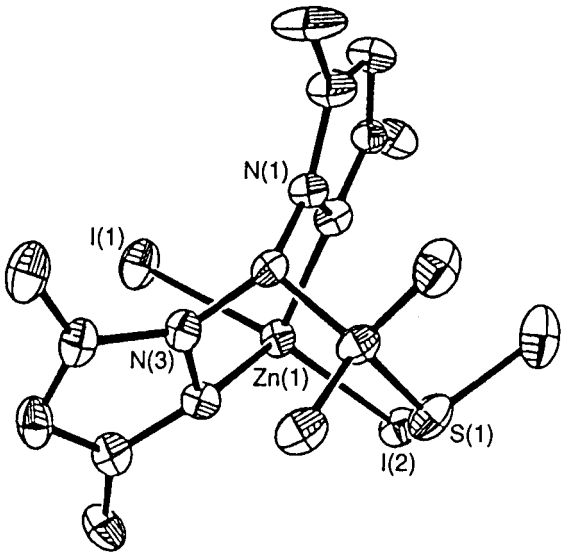

Figure 2. ORTEP diagram with 30% thermal ellipsoids for [(L3SCH$_3$)-ZnI$_2$] showing atomic labeling for the coordination sphere only. Hydrogen atoms are omitted for clarity.

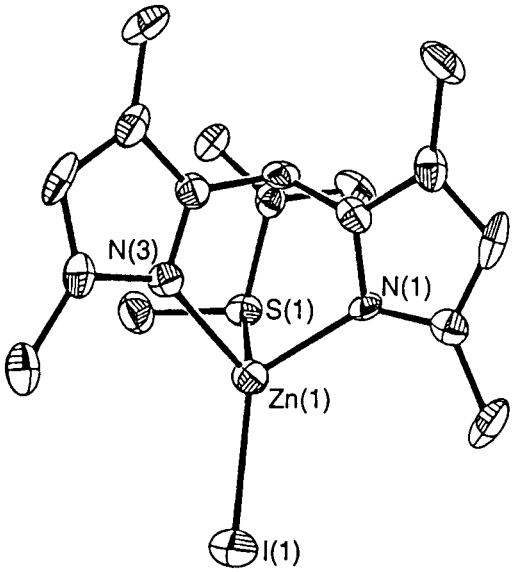

Figure 3. ORTEP diagram with 30% thermal ellipsoids for the cationic portion of [(L3SCH$_3$)ZnI]BF$_4$ showing atomic labeling for the coordination sphere only. Hydrogen atoms are omitted for clarity.

for idealized trigonal bipyramidal geometry. This deviation results from the small bite angle of the tridentate ligand (L3SCH$_3$). The metal ion lies only slightly below (0.15 Å) the trigonal plane formed by the pyrazolyl nitrogens and thiolate sulfur toward the thioether sulfur S(1). The apical sulfur S(1) is positioned perpendicular to the trigonal plane, resulting in an average $N_{pz}-Zn(1)-S(1)$ and $S(1)-Zn(1)-S(2)$ bond angles of 86.77° and 104.4°, respectively. The $Zn(1)-S_{thioether}$ bond length of 2.563(2) Å in $[(L3SCH_3)ZnSPh^{F5}]^+$ is considerably longer than other reported zinc−thioether complexes with pseudotetrahedral geometry and shorter than bond lengths seen in octahedral complexes (avg. 2.62(1) Å [(L3SCH$_3$)Zn-μ-bis-acetato-μ-hydroxo-Zn(L3SCH$_3$)]$^+$ and [(L3SCH$_3$)$_2$Zn]$^{2+}$, consistent with **7** being described as a five coordinate trigonal bipyramidal zinc complex. A rather strongly bound perchlorate oxygen located *trans* to the apical thioether sulfur with a S(1)−Zn(1)−O(1) bond angle of 175.12 (12)° and Zn(1)−O(1) bond distance of 2.527(5) Å completes the coordination sphere.

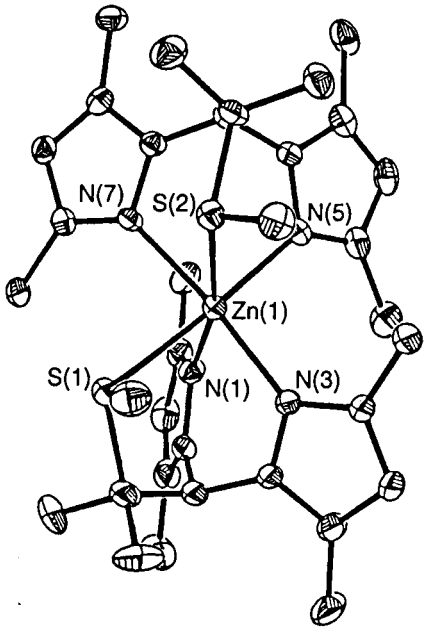

Figure 4. ORTEP diagram with 30% thermal ellipsoids for the cationic portion of [(L3SCH$_3$)$_2$Zn][BF$_4$]$_2$ showing atomic labeling for the coordination sphere only. Hydrogen atoms are omitted for clarity.

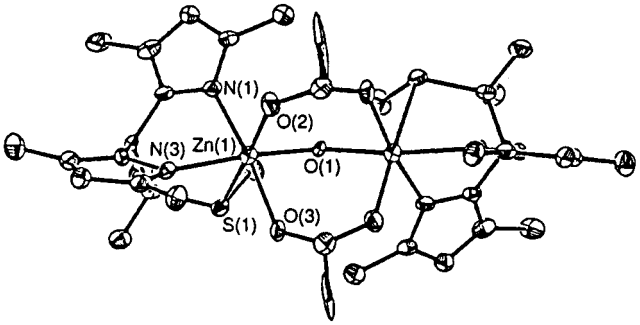

Figure 5. ORTEP diagram with 30% thermal ellipsoids for the cationic portion of [(L3SCH$_3$)Zn-μ-bis-acetato-μ-hydroxo-Zn(L3SCH$_3$)]BF$_4$ showing atomic labeling for the coordination sphere only. Hydrogen atoms are omitted for clarity.

Synthesis and Reactivity. Pseudotetrahedral zinc complexes such as [(L3S)ZnI] **1**, [(L3S)ZnOAc], or [(L3S)ZnSPh^{F5}], were readily prepared by either direct reaction of deprotonated (L3S)$^-$ (methoxide ion) with the appropriate zinc salt or protonation of the [(L3S)ZnCH$_3$] derivative with HX. Although methylation of the coordinated thiolate in these complexes could be achieved using methyl iodide, trimethyloxonium tetrafloroborate, or *p*-nitrobenzenesulfonic acid methyl ester as methyl donors, slightly different results ensued depending on the coordinating properties of the products.

Reaction of **1** with 1 equiv of methyl iodide in dichloromethane yields the complex [(L3SCH$_3$)ZnI$_2$], **2**, where the thioether is uncoordinated as has been previously found in all related systems. Reasoning that the neutral thioether could not compete with the anionic iodide ion released in the methylation reaction, we removed one iodide by treatment of **2** with 1 equiv of AgBF$_4$ or AgClO$_4$. Isolation of the product after filtration of precipitated AgI yielded the desired pseudotetrahedral complex **3**, [(L3SCH$_3$)ZnI]$^+$, where the thioether is now bound to the zinc. Addition of a second equivalent of AgBF$_4$ yields what we believe to be the dication, **4**, [(L3SCH$_3$)Zn(ACN)$_3$]$^{2+}$. These transformations are summarized in Scheme 1. Although crystals of **4** were forthcoming, they diffracted too poorly to be of use;

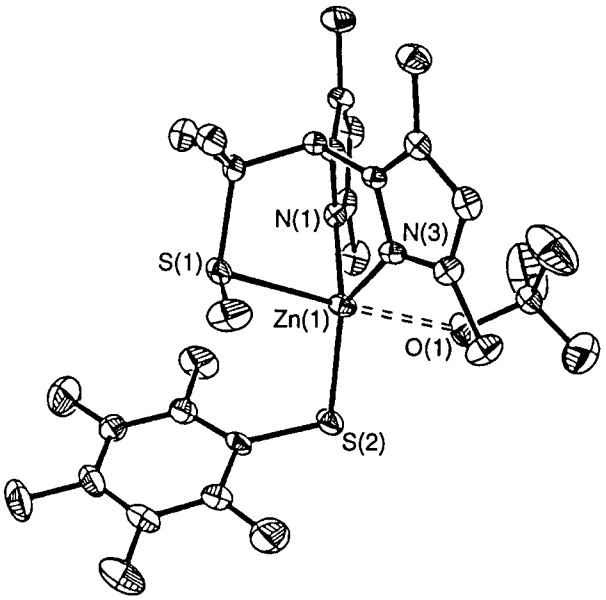

Figure 6. ORTEP diagram with 30% thermal ellipsoids for the cationic portion of $[(L3SCH_3)ZnSPh^{F5}]ClO_4$ showing atomic labeling for the coordination sphere only. Hydrogen atoms are omitted for clarity.

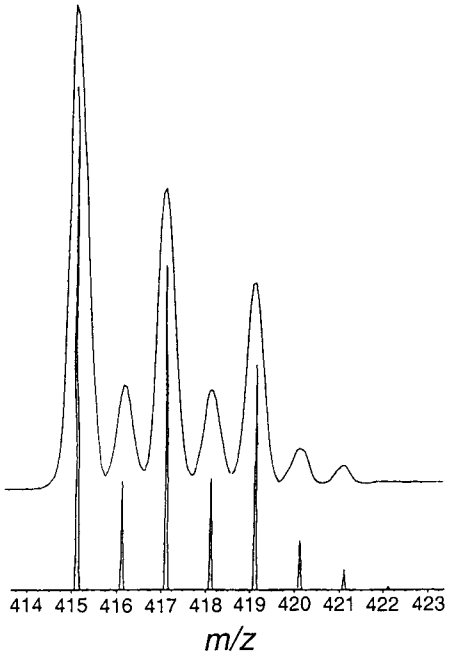

Figure 7. Observed (upper) and calculated (lower) ESI-MS isotope distribution pattern for the parent ion of $[(L3SCH_3)ZnOAc]^+$.

Scheme 1

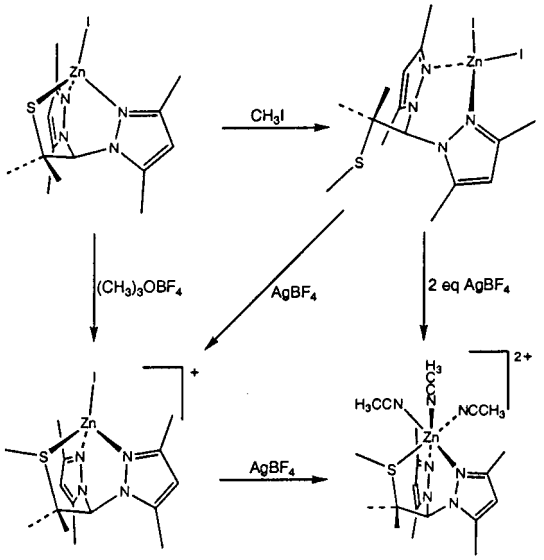

thus, we had to resort to more indirect methods for structural characterization. The ^{13}C chemical shift of a coordinated thioether methyl in our crystallographically characterized complexes is in the 14−15 ppm range which is a coordination-induced shift (CIS) of some 2−3 ppm over that for an unbound thioether methyl (11−12 ppm). The corresponding ^{13}C signal in **4** is at 14.7 ppm, strongly suggesting that the thioether sulfur is bound. IR confirms the presence of coordinated acetonitrile at 2280 cm^{-1} while no bands corresponding to simple lattice solvent are observed. The above and the analytical formulation of **4** as $L3SCH_3Zn{\cdot}3ACN{\cdot}H_2O$ lead us to favor an octahedral structure for the dication rather than tetrahedral, but definitive proof will require better crystals.

Since the iodide ion in **3** is not a biologically relevant ligand, we examined the methylation of the acetate complex, [(L3S)-Zn(OAc)]. The same reaction sequence leads to what we presume to be $[(L3SCH_3)ZnI(OAc)]$ with a pseudotetrahedral geometry and an uncoordinated thioether, although we have not isolated and characterized this species. Removal of the iodide

Scheme 2

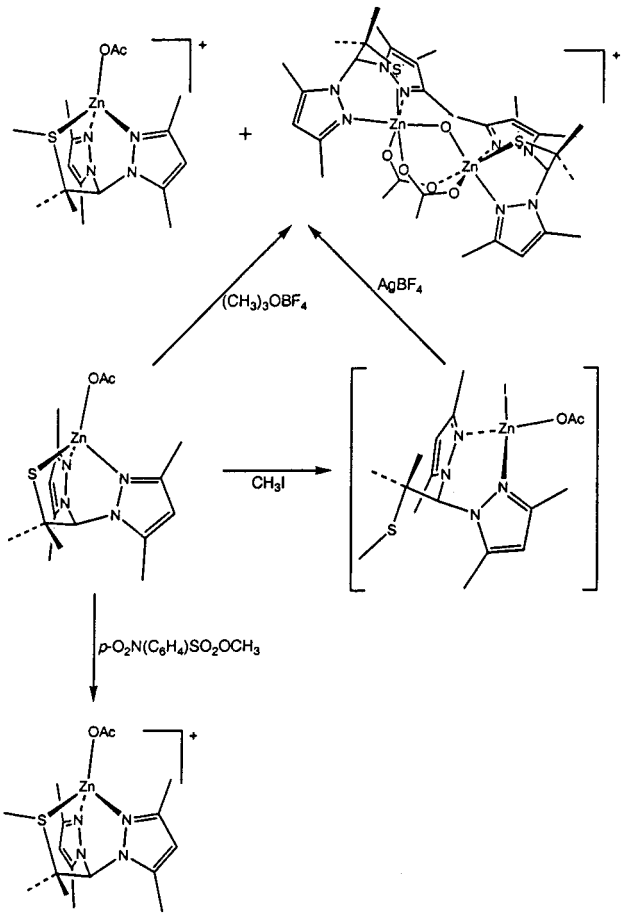

with $AgBF_4$ leads in solution to $[(L3SCH_3)ZnOAc]^+$ (Scheme 2). Both NMR and ESI-MS (Figure 7) are consistent with the formation of the psuedotetrahedral cation, $[(L3SCH_3)ZnOAc]^+$, which is expected to be isostructural with **3**. However, due to the propensity of the acetate group to bridge, another species was also detected in solution (NMR and ESI-MS), i.e., the

dimerization product, $[(L3SCH_3)Zn\text{-}\mu\text{-bis acetato-}\mu\text{-hydroxo-}Zn(L3SCH_3)]^+$ (**5**). In the solid state, **5** (containing octahedral zinc with coordinated thioethers) is the only species observed. Presumably **5** is the least soluble component of the mixture and crystallizes first, pulling the equilibrium completely in that direction. That the monomer and dimer are in fact in equilibrium in solution was revealed when some of the crystals containing only **5**, as determined by X-ray analysis, were dissolved in acetonitrile whereupon peaks assignable to both are observed by ^{1}H NMR.

Together, these results show clearly that in the absence of superior *anionic* ligands, such as iodide, neutral thioethers can bind to a zinc center in either a tetrahedral or octahedral geometry. Although coordinated thioether complexes could be prepared by removal of iodide by treatment with silver salts, the question remained, would a thioether formed by methylation of a zinc-bound thiolate remain coordinated without outside intervention? Trimethyloxonium tetrafloroborate and *p*-nitrobenzenesulfonic acid methyl ester are methyl donors used extensively to modify cysteine residues in proteins and are expected to produce only the weakly coordinating CH_3OCH_3 or *p*-nitrobenzene sulfonic acid as byproducts. Reaction of [(L3S)-ZnOAc] with either of the above gave the expected $[(L3SCH_3)$-$ZnOAc]^+$ directly, but the degree of dimerization of the latter to **5** seems to be highly anion dependent. Thus, while the BF_4^- salt, derived from using trimethyloxonium tetrafloroborate as a methylating agent, gave the expected equilibrium mixture of monomer and dimer in solution (from which solution only dimer crystallizes), the *p*-nitrobenzenesulfonate salt showed only monomer in both the solid state (as determined by elemental analysis) and solution (NMR and ESI-MS).

Since most of the metal binding sites in the zinc-containing enzymes involved in alkyl group transfer contain more than one cysteine thiolate, it is important to determine how reactivity can be controlled to allow for the alkylation of a single such ligand. To model this situation, we attempted to methylate the complex, $[(L3S)ZnSPh^{F5}]$, which contains two thiolate sulfurs. Our previous mechanistic work has shown that the rate of methylation of zinc-bound thiolates was linearly related to the pK_a of the free thiol.[19] Thus pentaflorothiophenolate was expected to react orders of magnitude slower than the alkyl thiolate in $[(L3S)ZnSPh^{F5}]$, suggesting that clean methylation of just one of the two thiolate sulfurs was possible. This indeed proved to be the case. Reaction of $[(L3S)ZnSPh^{F5}]$ with 1 equiv of CH_3I followed by addition of 1 equiv of $AgClO_4$ readily produced the desired $[(L3SCH_3)ZnSPh^{F5}]ClO_4$. Mixed thiolate, thioether coordination of zinc is rare, but at least two examples are known.[17,20] Compound **7** is also of interest in that it contains a binding site remarkably similar to that found in azurin, i.e., two histidine nitrogens (ca. 2.0 Å), a thioether from methionine (3.1−3.3 Å), a thiolate sulfur of cysteine (2.14 Å), and a glycine carbonyl (2.7−3.1 Å) in a trigonal bipyramidal arrangement.[21] Zn-substituted azurin has a similar structure but shows a shortening of the metal carbonyl interaction to 2.3 Å and a lengthening of the thioether sulfur−metal interaction to 3.4 Å to give a more pseudotetrahedral array.[22] Interestingly compound

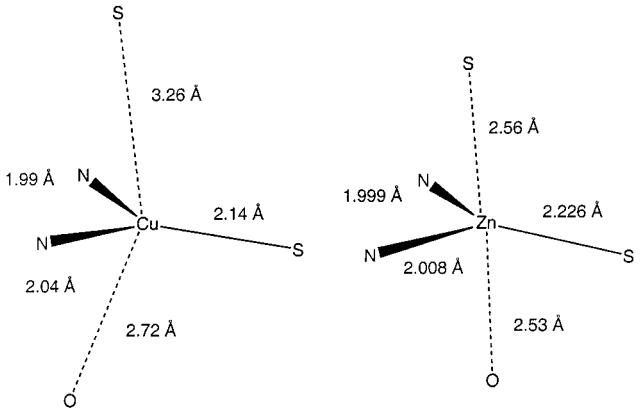

7 has a much stronger interaction with the thioether sulfur than the protein and thus more closely resembles the native Cu binding geometry than that of the Zn-substituted azurin. If these differences are due to the constraints of the ligand in **7** is unclear. Model systems designed to mimic the active site of azurin have been sought for decades, but only recently has a well-characterized example emerged.[23] Thus it remains to be seen if isostructural complexes with metals of spectroscopically more interest than zinc (i.e., Cu, Ni, or Co) can be prepared, thus increasing the number of available model systems. If so, the zinc complex **7** would make an ideal diamagnetic host in which to conduct detailed EPR investigations.

Discussion

The work on the model system reported herein was undertaken in the hope that it would mimic some of the chemistry of zinc enzymes involved in alkyl group transfer. Questions of interest to both inorganic and biochemists include the following: (1) What role does the zinc play in modulating the nucleophilicity of a cysteine thiolate? (2) How can the reactivity of a specific cysteine be controlled when more than one is bound to a zinc center? (3) Why has nature chosen a thiol-rich coordination environment for the zinc in these proteins? (4) How does alkylation of a cysteine affect its ability to bind to zinc? Our initial mechanistic studies have confirmed that a zinc-bound thiolate is the likely active nucleophile in such systems and have shed some light on questions two and three as well.[19]

In the present work we have sought to examine the coordination properties of thioethers formed by alkylation of a thiol. While a number of zinc thioether complexes are known,[15−17,20] and strong evidence for coordination of thioethers has been presented for enzymes such as Ada and farnasyl transferase,[11−13] attempts to produce bound thioethers via alkylation of a zinc-bound thiolate in model systems have consistently failed.[7−9,24−26]

Previous work has shown that charge and structure are important considerations in the coordination (or lack thereof) of thioethers to zinc. Thus, thioethers as part of *anionic chelates* are very good ligands indeed, as shown by the seminal work of Riorden, Darensbourg, and Parkin.[15−17,20] Numerous *neutral* chelates containing thioethers, on the other hand, have also been examined, and in these cases the thioethers were invariably *uncoordinated*.[24,25,27−29] However, the thioether in these systems was generally competing with various anionic ligands (i.e.,

(19) Hammes, B. S.; Warthen, C. R.; Crans, D. C.; Carrano, C. J. *J. Biol. Inorg. Chem.* **2000**, *6*, 82.
(20) Goodman, D. C.; Tuntulani, T.; Farmer, P. J.; Darensbourg, M. Y.; Reibenspeis, J. H. *Angew. Chem., Int. Ed. Engl.* **1993**, *32*, 116.
(21) Holm, R. H.; Kennepohl, P.; Solomon, E. I. *Chem. Rev.* **1996**, *96*, 2239.
(22) Nar, H.; Huber, R.; Messerschmidt, A.; Fillipou, A. C.; Barth, M.; Jacquinod, M.; van de Kamp, M.; Canters, G. W. *Eur. J. Biochem.* **1992**, *205*, 1123.
(23) Holland, P. L.; Tolman, W. B. *J. Am. Chem. Soc.* **2000**, *122*, 6331.
(24) Roehm, P. C.; Berg, J. M. *J. Am. Chem. Soc.* **1998**, *120*, 13083.
(25) Grapperhaus, C. A.; Tuntulani, Reibenspies, J. H.; Darensbourg, M. Y. *Inorg. Chem.* **1998**, *37*, 4052.
(26) Bridgewater, B. M.; Fillebeen, T.; Friesner, R. A.; Parkin, G. *J. Chem. Soc., Dalton Trans.* **2000**, 4494.
(27) Gregorzik, R.; Vahrenkamp, H. *Chem. Ber.* **1994**, *127*, 1857.

Cl^-,Br^-, or I^-) derived from the initial metal salt used. In only one case was an attempt made to remove the halide by silver abstraction or to utilize zinc salts containing noncoordinating counterions which again failed to yield coordinated thioether.[25] The ligands used in many of these previous studies tended to adopt either a meridonal (T-shaped) geometry or were so stericly restricted that they enforced square planar or square pyramidal geometries. These geometries are neither ideal for zinc nor representative of the binding sites in zinc metalloproteins. Hence, it clear that *neutral* thioethers cannot, in general, compete with anionic ligands, particularly in nonoptimal geometries. In our work, the facially coordinating nature of our ligands tends to promote a tetrahedral geometry, and neutral thioethers as part of such a scaffold appear to bind zinc quite well in the absence of superior anionic ligands. The fact that the thioether that is not bound in **2** spontaneously moves into the coordination sphere when the iodide is removed as in **3** shows that a special, sterically restricted protein environment is not necessary to support thioether coordination.

We have also been able to validate the suggestion, based on our previous work, that reactivity of a single thiolate in a multithiolate binding site could be controlled by differences in pK_a.[19] In native proteins the pK_a of the various thiolates can be influenced by a variety of factors including electrostatic and/or hydrogen bonding interactions. Thus, for example, the periplasmic mercuric ion-binding protein (merP) contains two essential cysteine residues with widely different pK_a's of 5.5 and 9.16.[30] The low pK_a of one of these is attributed to the presence of a nearby, negatively charged residue. Such a pK_a difference is not unlike that found in our model complex, [(L3S)-ZnSPh^{F5}]. A similar situation in zinc-containing alkyl transfer enzymes could well render one cysteine residue far more reactive than the others. Of course steric factors may also play an important role as well.

Finally, it is worth noting that the chelate effect is obviously important in helping the thioether group remain coordinated to a metal such as zinc. Indeed, a simple neutral monodentate thioether is an unlikely ligand, and to the best of our knowledge no such complex has been reported. Thus, we can envision zinc enzymes involved in alkyl group transfer as being divided into two groups: the first where the sulfur to be alkylated is part of the protein backbone, i.e., one of the cysteine donors in the zinc coordination sphere as in the Ada protein. Under these conditions, the resulting thioether can be expected to remain coordinated to the zinc due to the macromolecular chelate effect. In the case where the thiol to be alkylated represents an exogenous substrate, as in the methionine synthases, the resulting *neutral monodentate* coordinated thioether is expected to be easily displaced by other ligands such as water (or hydroxide). Such a process would yield free product and zinc enzyme with an open coordination site ready to repeat the catalytic cycle.

Acknowledgment. This work was supported in part by Grants AI-1157 from the Robert A. Welch Foundation and CHE-9726488 from the NSF. The NSF-ILI program grant USE-9151286 is acknowledged for partial support of the X-ray diffraction facilities at Southwest Texas State University.

Supporting Information Available: Complete listings of atomic positions, bond lengths and angles, anisotropic thermal parameters, hydrogen atom coordinates, data collection and crystal parameters, and ORTEP diagrams for all crystallographically characterized complexes. This material is available free of charge via the Internet at http://pubs.acs.org.

IC001178P

(28) Matthews, C. J.; Clegg, W.; Heath, S. L.; Martin, N. C.; Hill, M. N.; Lockhart, J. C. *Inorg. Chem.* **1998**, *37*, 199.
(29) Ghosh, P.; Wood, M.; Bonanno, J. B.; Hascall, T.; Parkin, G. *Polyhedron* **1999**, *18*, 1107.
(30) Powlowski, J.; Sahlman, L. *J. Biol. Chem.* **1999**, *274*, 33320.